

Article

Synthesis, Molecular Docking, and Neuroprotective Effect of 2-Methylcinnamic Acid Amide in 1-methyl-4-phenyl-1,2,3,6-tetrahydropyridine (MPTP)—An Induced Parkinson's Disease Model

Maya Chochkova ^{1,*}, Rusi Rusew ², Reni Kalfin ³, Lyubka Tancheva ³, Maria Lazarova ³, Hristina Sbirikova-Dimitrova ², Andrey Popatanasov ³, Krasimira Tasheva ⁴, Boris Shivachev ², Nejc Petek ⁵ and Martin Štícha ⁶

¹ Faculty of Mathematics and Natural Sciences, South-West University “Neofit Rilski”, 66 Ivan Mihailov Str., 2700 Blagoevgrad, Bulgaria

² Institute of Mineralogy and Crystallography “Akad. Ivan Kostov”, Bulgarian Academy of Sciences, Acad. G. Bonchev bl., 107 Sofia, Bulgaria

³ Institute of Neurobiology, Bulgarian Academy of Sciences, Acad. G. Bonchev Bl.23, 1113 Sofia, Bulgaria

⁴ Institute of Plant Physiology and Genetics, Bulgarian Academy of Sciences, 1113 Sofia, Bulgaria

⁵ Faculty of Chemistry and Chemical Technology, University of Ljubljana, Večna pot 113, 1000 Ljubljana, Slovenia

⁶ Section of Chemistry, Faculty of Science, Charles University, Hlavova 2030/8, 12843 Prague, Czech Republic

* Correspondence: mayabg2002@yahoo.com



Citation: Chochkova, M.; Rusew, R.; Kalfin, R.; Tancheva, L.; Lazarova, M.; Sbirikova-Dimitrova, H.; Popatanasov, A.; Tasheva, K.; Shivachev, B.; Petek, N.; et al. Synthesis, Molecular Docking, and Neuroprotective Effect of 2-Methylcinnamic Acid Amide in 1-methyl-4-phenyl-1,2,3,6-tetrahydropyridine (MPTP)—An Induced Parkinson's Disease Model. *Crystals* **2022**, *12*, 1518. <https://doi.org/10.3390/cryst12111518>

Academic Editor: Abel Moreno

Received: 8 September 2022

Accepted: 21 October 2022

Published: 26 October 2022

Publisher's Note: MDPI stays neutral with regard to jurisdictional claims in published maps and institutional affiliations.



Copyright: © 2022 by the authors. Licensee MDPI, Basel, Switzerland. This article is an open access article distributed under the terms and conditions of the Creative Commons Attribution (CC BY) license (<https://creativecommons.org/licenses/by/4.0/>).

Abstract: Parkinson's disease (PD) has emerged as the second most common form of human neurodegenerative disorders. However, due to the severe side effects of the current antiparkinsonian drugs, the design of novel and safe compounds is a hot topic amongst the medicinal chemistry community. Herein, a convenient peptide method, TBTU (O-(benzotriazole-1-yl)-N,N,N',N'-tetramethyluronium tetrafluoroborate), was used for the synthesis of the amide (*E*)-*N*-(2-methylcinnamoyl)-amantadine (CA(2-Me)-Am; 3)) derived from amantadine and 2-methylcinnamic acid. The obtained hybrid was studied for its antiparkinsonian activity in an experimental model of PD induced by MPTP. Mice (C57BL/6, male, 8 weeks old) were divided into four groups as follows: (1) the control, treated with normal saline (i.p.) for 12 consecutive days; (2) MPTP (30 mg/kg/day, i.p.), applied daily for 5 consecutive days; (3) MPTP + CA(2-Me)-Am, applied for 12 consecutive days, 5 days simultaneously with MPTP and 7 days after MPTP; (4) CA(2-Me)-Am +oleanoic acid (OA), applied daily for 12 consecutive days. Neurobehavioral parameters in all experimental groups of mice were evaluated by rotarod test and passive avoidance test. Our experimental data showed that CA(2-Me)-Am in parkinsonian mice significantly restored memory performance, while neuromuscular coordination approached the control level, indicating the ameliorating effects of the new compound. In conclusion, the newly synthesized hybrid might be a promising agent for treating motor disturbances and cognitive impairment in experimental PD.

Keywords: amantadine; 2-methylcinnamic acid; single crystal X-ray diffraction; Parkinson's disease

1. Introduction

Globally, the growth of the older population, comprising 7 % or more of the total population, is projected to reach about 2 billion people by 2050 [1]. Thereafter, this can be associated with increasing prevalence of age-related diseases as neurodegenerative diseases, such as Parkinson's disease and Alzheimer's disease, among others. According to the WHO (World Health Organization), amongst the neurological disorders, there is a growing concern around the disability and death caused by PD [2]. Parkinsonism is the second most common neurodegenerative disaster after Alzheimer's disease [3,4]. Currently,

there are no strategies that can stop the brain cell injury afflicted by PD. The multifactorial nature of this incurable pathology requires an effective multi-target concept that can hit diverse targets. However, the almost all of the central nervous system drug candidates do not efficiently penetrate the blood–brain barrier. Therefore, to solve this problem, it is widely accepted that the addition of a lipophilic rest to main structure can modify absorption, distribution, metabolism, or excretion (ADME) properties of an entire molecule.

Accordingly, adamantane core has been known as a precise building block that can alter the lipophilicity on a lead compound, without increasing its toxicity. Indeed, there are many adamantane-based compounds that are currently used in clinical practice and also as potential therapeutics [5,6]. However, the end of the era of aminoadamantanes, including rimantadine and amantadine as antiviral, is delineated, since they have faced increasing resistance against influenza A strains [7–9]. Surprisingly, a random finding resurrected the role of amantadine in the efficacy for symptomatic alleviation in PD [10], as well as for other movement disorders [11]. Additionally, the dual effects of amantadine on parkinsonian signs and symptoms and levodopa-induced dyskinesias are due to its dopaminergic and glutamatergic properties [11]. Amantadine is the only glutamate antagonist drug that is prescribed against PD, often used to treat dyskinesia. However, the clinical use of amantadine is limited because of concerns regarding its safety and tolerability issues, as well as the duration of its antidyskinetic efficacy. Hence, the search for new agents with powerful antiparkinsonian action and good biological tolerance is an important task for chemists and biologists.

In this regard, cinnamic acid (CA) has been known as a plant 3-phenylpropenoic acid and represents one of the constituents in the common spice cinnamon. This unsaturated carboxylic acid has been obtained through phenylpropanoid pathway as a deaminated plant product of its amino acid precursor phenylalanine. Besides having a plethora of activities such as antidiabetic [12] and anti-cancer [13] effects, cinnamic acid emerges with a new function in protecting dopaminergic neurons via PPAR α [14]. Moreover, an earlier result [15] reveals that cinnamic acid improves memory by suppressing the oxidative stress and cholinergic dysfunction in the brain of diabetic mice.

Inspired by the above-mentioned results for CA, in our study, we report the synthesis of a hybrid molecule consisting of methylated cinnamic acid and amantadine. Furthermore, the newly obtained derivative was examined as a potential neuroprotective agent in the MPTP experimental mouse model of PD.

2. Materials and Methods

2.1. General Methods

2-Methyl-cinnamic acid, amantadine, and other reagents were purchased from Angene Chemical, Sigma Aldrich (FOT, Bulgaria), whereas all solvents were obtained from Thermo Fisher Scientific (Bulgaria) and applied with no further purification. Thin-layer chromatography (TLC) was carried out on precoated Kieselgel 60F₂₅₄ plates (Merck, Germany) with detection by UV absorbance at 254 nm. A TLC plate was visualized by Ce-PMo reagent solution followed by heating. Flash chromatography of the target amide was performed on prepackaged BÜCHI FlashPure EcoFlex silica columns.

The newly amide 3 was synthesized according to the modified literature method [16]. The NMR spectra were recorded in deuterated solvents with (CH₃)₄Si as the internal standard on a Bruker Ascend neo NMR 600 instrument (Bruker, Billerica, MA, USA) at 600 MHz for ¹H nuclei and at 151 MHz for ¹³C nuclei. A Bruker Compact QTOF-MS (Bruker Daltonics, Bremen, Germany) controlled by the Compass 1.9 Control software was used to measure the mass spectrum. The monoisotopic mass values were calculated using Data analysis software v 4.4 (Bruker Daltonics, Germany). The analysis was conducted in the positive ion mode at a scan range from m/z 50 to 1000, and nitrogen was used as nebulizer gas at a pressure of 4 psi and flow of 3 L/min for the dry gas. The capillary voltage and temperature were set at 4500 V and 220 °C, respectively.

2.2. Synthesis of (E)-N-(2-Methylcinnamoyl)-Amantadine (3)

2-Methylcinnamic acid (1.8 g, 11.4 mmol) was suspended in 30 mL of CH₂Cl₂, and then, after adding Et₃N (1.6 mL, 11.4 mmol), the obtained colorless liquid was treated by solid TBTU (3.7 g, 11.4 mmol). After being stirred for ≈10 min, to the mixture, we added amantadine (2.4 g, 12.6 mmol) and Et₃N (1.8 mL, 12.6 mmol), dissolved (under sonication) in 40 mL CH₂Cl₂. Thus, the reaction mixture was stirred at room temperature for 3 h, and then was diluted with an additional 30 mL CH₂Cl₂. The organic phase was washed with 5% aqueous NaHCO₃ (5 × 50 mL) and brine (3 × 50 mL), dried over Na₂SO₄, and concentrated in vacuo. Furthermore, after purification, the amide was obtained (3.3 g, 89%) as white crystals.

Compound (3): white crystals (CH₃CN); mp 188–189 °C; ¹H NMR (DMSO-d₆, 600 MHz) δ 7.59 (s, 1H), 7.56 (d, J = 15.6 Hz, 1H), 7.48 (d, J = 7.3 Hz, 1H), 7.27–7.20 (m, 3H), 6.58 (d, J = 15.6 Hz, 1H), 2.35 (s, 3H), 2.03 (bs, 3H), 2.00 (bs, 6H), 1.64 (bs, 6H); ¹³C NMR (DMSO-d₆, 151 MHz) δ 164.5, 137.0, 135.7, 134.4, 131.1, 129.4, 126.8, 126.3, 125.3, 51.4, 41.5, 36.5, 29.3, 19.9; HRMS m/z 318.1830 (calcd for C₂₀H₂₅NNaO, 318.1828).

2.3. Single Crystal X-ray Diffraction (SCXRD) of (E)-N-(2-methylcinnamoyl)-amantadine (3)

Single crystals of compound 3 were grown from 1:1 v/v benzene methanol solution. A crystal with suitable size and quality was selected and was mounted on a glass capillary. The diffraction peak intensities and coordinates were collected on Bruker D8 Venture diffractometer (Bruker AXS GmbH, Karlsruhe, Germany) equipped with a PhotonII CMOS detector using micro-focus MoKα radiation (λ = 0.71073 Å). Data were processed with CrysAlisPro software [17]. The structure was solved with intrinsic methods using ShelxT [18] and refined by the full-matrix least-squares method on the F² with ShelXL program [19]. All non-hydrogen atoms were located successfully from the Fourier map and were refined anisotropically. Hydrogen atoms were placed on calculated positions (C–H_{aromatic} = 0.93, C–H_{methyl} = 0.96 Å, and C–H_{methylene} = 0.97 Å, riding on the parent atom (U_{eq} = 1.2). The H atom near the nitrogen was located from a different Fourier map. Complete crystallographic data for the structure of the title compound reported in this paper were deposited in the CIF format at the Cambridge Crystallographic Data Center as 2205297. These data can be obtained free of charge via <http://www.ccdc.cam.ac.uk/conts/retrieving.html>, deposited on 5 September 2022 (or from the CCDC, 12 Union Road, Cambridge CB2 1EZ, UK; Fax: +441223336033; e-mail: deposit@ccdc.cam.ac.uk).

2.4. Neurobehavioral Studies

Mice (C57BL/6, male, 8 weeks old) were obtained from Erboj (Animal Breeding Center, Slivniza, Sofia). The animals were housed two per cage under constant laboratory conditions (25 ± 3°C, 12/12 h light/dark cycle) with food and water available ad libitum. The habituation period was 5 days before the start of the experiment. The protocol of all experiments was in accordance with the requirements of the European Communities Council Directive 86/609/EEC and rules of the Bioethics Committee 30/03/2021, Institute of Neurobiology, Bulgarian Academy of Sciences.

CA(2-Me)-Am (3) was dissolved in oleanolic acid (OA). We tested five doses of amide 3 applied per os on 25 male mice C57BL/6 and found the dose of 20 mg/kg to be the most effective.

Mice were divided into four experimental groups (n = 8 in each group) as follows: (1) control, treated with normal saline (i.p.) for 12 consecutive days; (2) MPTP (30 mg/kg/day, i.p.) applied daily for 5 consecutive days in accordance with the work of Shin et al. [20]; (3) MPTP (30 mg/kg, i.p.) + CA(2-Me)-Am (20 mg/kg, per os) applied for 12 consecutive days, 5 days simultaneously with MPTP and 7 days after MPTP; (4) MPTP (30 mg/kg, i.p.) + OA (per os) applied daily for 12 consecutive days.

All mice training was conducted before MPTP administration.

2.4.1. Rotarod Test

Mice from all experimental groups were placed on a gyrotory with a fixed speed of 7 rpm/min, and the time on rotarod was determined. The observation period was 5 min. All animals were pre-trained on the rotarod apparatus before treatment in order to reach stable performance. The training consisted of one session per day over 3 consecutive days. The test was made on the 13th day, and the average time per group was calculated after the experiment and repeated four times [21].

2.4.2. Passive Avoidance Test

Learning and memory performance in mice was evaluated using passive avoidance learning test [22]. Acquisition phase: during this phase, each animal was placed in the illuminated compartment. When the rodents innately entered into the dark compartment, they received a mild electrical foot shock (0.5 mA, 3 s). In this trial, the initial latency (IL) of entrance into the dark chamber of each animal was recorded, and mice with ILs > 60 s were excluded from the study. Test phase: on the 13th and 14th days, each mouse was placed in the illuminated chamber, and the entry into the dark chamber was measured as step through latency (STL). The behavioral observations were carried out between 9 a.m. and 12 a.m.

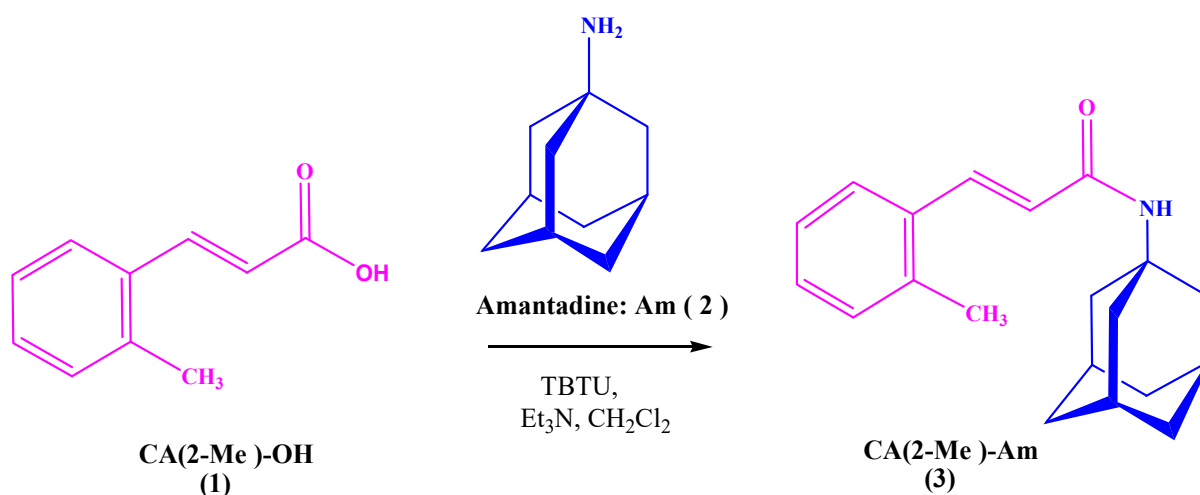
2.4.3. Statistical Analysis

The results were expressed as means \pm the standard error of the mean (SEM) or as percentage changes over the mean compared to the control. Statistical analyses of the data were performed by one-way analysis of variance (ANOVA) followed by Dunnett post hoc comparison test. Differences were considered significant at $p < 0.05$.

3. Results and Discussion

3.1. Chemistry

Herein, the 2-methylcinnamic acid amide (CA(2-Me)-Am; 3) was synthesized as outlined in Scheme 1. Generally, the amidation of 2-methylcinnamic acid (CA(2-Me)-OH; 1) with amantadine (Am; 2) was carried out in the presence of tertiary amine (triethylamine, Et₃N) and by one of the preferred coupling reagents for in situ activation, such as TBTU [16] to amide 3.



Scheme 1. Synthetic route of amide 3.

The structure of the newly obtained compound (3) was confirmed by the ¹H NMR, ¹³C NMR, HRMS, and single crystal analysis powder diffraction. The title compound (CA(2-Me)-Am; 3) crystallized in the monoclinic *P*2₁/*c* space group, with one molecule in the asymmetric unit (Figure 1). The bond distances and angles (Table 1) within the

adamantane and 2-methylcinnamic acid were comparable with those observed in other structures [23–27].

Table 1. The most important data collection and crystallographic refinement parameters for (*E*)-*N*-(2-methylcinnamoyl)-amantadine.

Empirical formula	C ₂₀ H ₂₅ NO
Formula weight	295.41
Temperature/K	290.00
Crystal system	monoclinic
Space group	P2 ₁ /c
a/Å	14.692(2)
b/Å	11.900(2)
c/Å	9.9904(18)
α/°	90
β/°	104.943(5)
γ/°	90
Volume/Å ³	1687.6(5)
Z	4
ρ _{calc} /g/cm ³	1.163
μ/mm ⁻¹	0.071
F(000)	640.0
Crystal size/mm ³	0.3 × 0.25 × 0.2
Radiation	MoKα (λ = 0.71073)
2θ range for data collection/°	4.466 to 52.842
Index ranges	-18 ≤ h ≤ 17, -14 ≤ k ≤ 12, -12 ≤ l ≤ 12
Reflections collected	10,910
Independent reflections	3443 (R _{int} = 0.0595, R _{sigma} = 0.0654)
Data/restraints/parameters	3443/0/205
Goodness-of-fit on F ²	1.018
Final R indexes (I > =2σ (I))	R ₁ = 0.0605, wR ₂ = 0.1171
Final R indexes (all data)	R ₁ = 0.1142, wR ₂ = 0.1405
Largest diff. peak/hole/e Å ⁻³	0.17/−0.13

The angle between the phenyl and acrylamide moieties was 29.8 °, disclosing that the conjugation was not stringent, e.g., the conjugation could be disrupted. In the molecule of (*E*)-*N*-(2-methylcinnamoyl)-amantadine, one hydrogen donor (N–H) and one acceptor (carbonyl oxygen) were present. In the crystal structure, the molecules produced one-dimensional chains with a graph set C₁¹(4) [28,29] (Figure 2a). The three-dimensional packing of the molecules (Figure 2b) did not reveal additional weak interactions, and thus the stabilization of the crystal structure was achieved by the N1–H1 ... O1 hydrogen bond (N1 ... O1 of 3.065(5) Å).

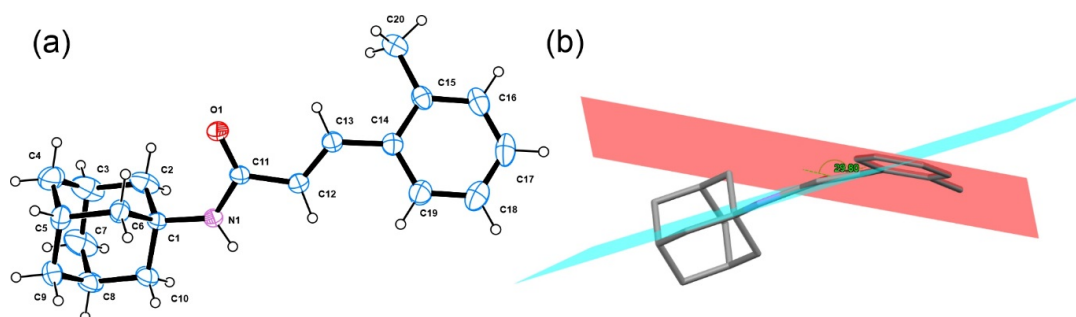


Figure 1. (a) ORTEP [30] view and numbering scheme of the molecule present in the asymmetric unit of (*E*)-*N*-(2-methylcinnamoyl)-amantadine; the thermal ellipsoids were drawn with 50% probability, and hydrogen atoms are shown as small spheres with arbitrary radii. (b) Observed angle between the mean plane of the phenyl (C1/C15/C16/C17/C18/C19) and acrylamide (C13/C12/C11/O1/N1) moieties (C13/C12/C11/O1/N1).

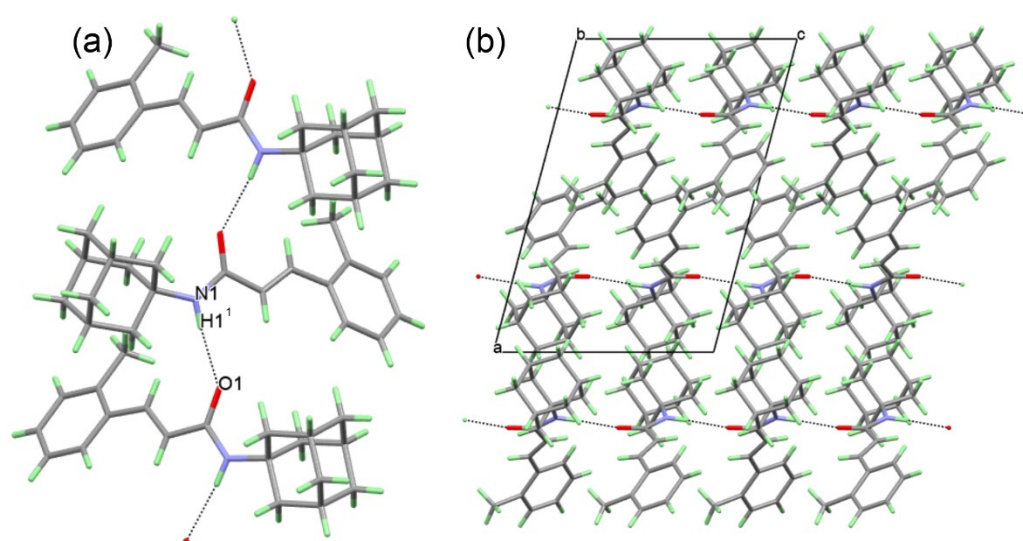


Figure 2. The observed (a) hydrogen bonding interaction stabilizing the crystal structure of (*E*)-*N*-(2-methylcinnamoyl)-amantadine and (b) a view along the *b* axis of the three-dimensional packing of the molecules and formation of $C_1^1(4)$ chains propagating along the [10] plane.

3.2. *In Vivo* Evaluation of Amide 3 in an Experimental Mouse Model of PD

3.2.1. Effect of CA(2-Me)-Am (3) on the Weight of Experimental Animals

There was no significant change in the weight of the control mice over the 12-day period. In those treated with MPTP, we observed a 6.92% weight gain within the group. In the MPTP + CA(2-Me)-Am and MPTP + OA mice, weight reduction was recorded at the end of the observed period at 17.41% and 15.51%, respectively (Figure 3).

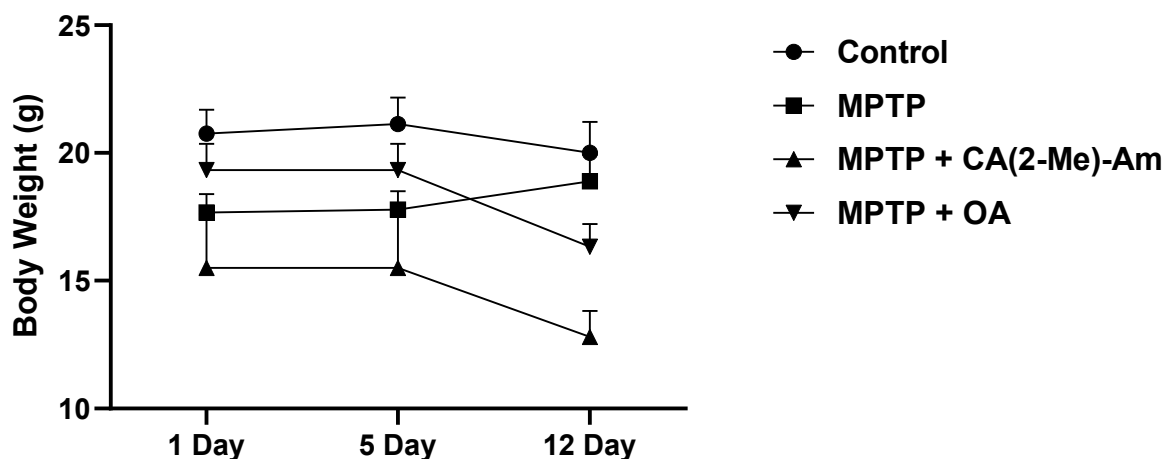


Figure 3. Effect of CA(2-Me)-Am on the weight of the experimental animals. Data are presented as means with their respective standard errors ($m \pm \text{S.E.M}$; $n = 8$; $* p < 0.05$).

3.2.2. Rotarod Test

The studies performed demonstrated that the group of mice treated either with the MPTP toxin or with MPTP + OA spent less time on the rotating lever of the rotarod apparatus as compared to the controls, which is an indication of a motor-impairing effect. The reduction was by 21.13 % ($p < 0.05$) for the MPTP group, and by 20.99 % ($p < 0.05$) for the MPTP + OA group (Figure 4). In the MPTP + CA(2-Me)-Am group, the time that experimental animals spent on the rotary lever was comparable to that of the control group (Figure 4).

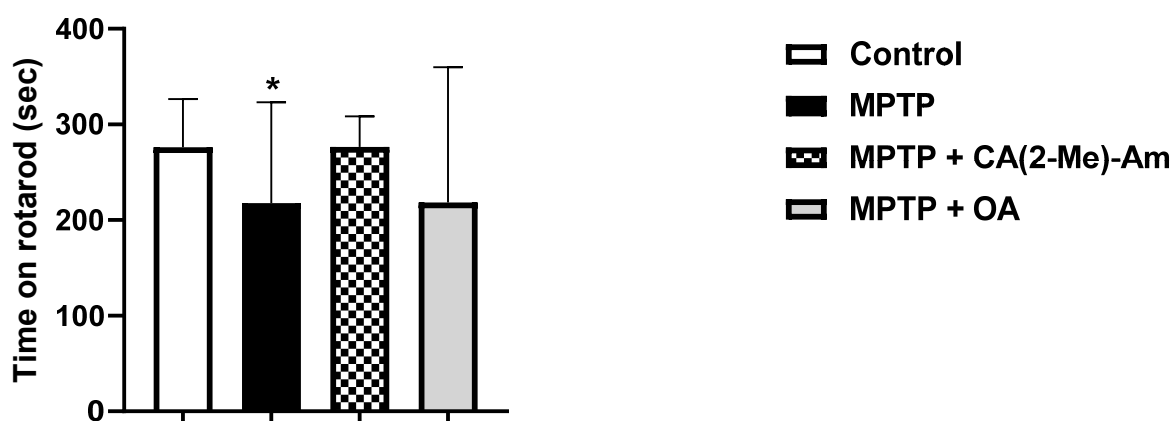


Figure 4. Effect of CA(2-Me)-Am on neuromuscular coordination. The asterisks above bars indicate significant differences in number of falls per minute for each experimental group versus the control at * $p < 0.05$. Statistical analysis was performed by one-way analysis of variance (ANOVA) followed by Dunnett's post hoc comparison test.

3.2.3. Passive Avoidance Test

The administration of the MPTP toxin caused a decrease in the step-through latency time by 31.56% ($p < 0.01$) at 1st h and by 33.45% ($p < 0.01$) at 24th h after the training of mice as compared to controls, which is evidence of memory and learning deficits. Administration of CA(2-Me)-Am increased the latent reaction time by 33.49% ($p < 0.05$) at the 1st h and by 33.84% ($p < 0.05$) at 24th h as compared to the MPTP-treated group, an indication of a memory-protective effect of the newly synthesized amantadine derivative (Figure 5).

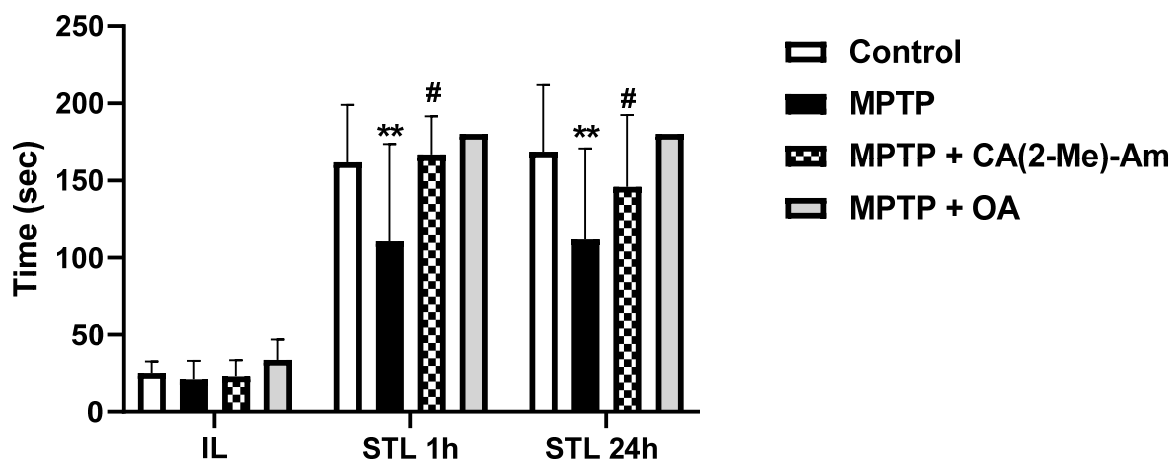


Figure 5. The effect of CA(2-Me)-Am on initial latency (IL) and step-through latency (STL) in a single-trial passive avoidance test in a mouse model of PD. Significance vs. control group: ** $p < 0.01$; significance vs. MPTP-treated group: # $p < 0.05$. Statistical analysis was performed by one-way analysis of variance (ANOVA), followed by Dunnett's post hoc comparison test.

3.3. Molecular Docking

The docking of (*E*)-*N*-(2-methylcinnamoyl)-amantadine (**3**) was performed against four different targets associated with PD: A_{2a}AR (3EML) [31], COMT (1H1D) [32], MAO-B (2C65) [33], and NMDA (7SAD) [34] (Table 2).

Table 2. Molecular docking score (kcal/mol) of (*E*)-*N*-(2-methylcinnamoyl)-amantadine against selected targets associated with PD.

	Molegro Virtual Docker Score	Detected Hydrogen Bonding Interaction
(<i>E</i>)- <i>N</i> -(2-methylcinnamoyl)- amantadine		
NMAD (7SAD) [34]	-80.240	No
COMT (1H1D) [32]	-111.957	No
A2aAR (3EML) [31]	-83.578	C=O ... O-H Tyr271 D ... A 3.38 Å
MAO-B (2C65) [33]	-119.889	C=O ... N-H Gly58 D ... A 3.09 Å

NMAD, *N*-methyl-*D*-aspartate receptor; COMT, catechol-*O*-methyltransferase; A2aAR, A2A adenosine receptor; MAO-B, monoamine oxidase B.

The docking approach involved predicting the conformation and orientation of ligands within a targeted binding site. Initially, the reference drug memantine present in 7SAD [34] was employed to adjust the docking parameters. The structures of the target enzymes were obtained from the Protein Data Bank (PDB), the coordinates of the small molecules were generated from the crystal structure of the (*E*)-*N*-(2-methylcinnamoyl)-amantadine, and positioning in the active site and docking were conducted using Molegro Virtual Docker (MVD2019.7.0.0-2019-03-18-1B win32). Details regarding the docking validation are provided in Figures S4 and S5. The UCSF Chimera [35] and Ligplot+ 2.2.5 [36] were used for visualization and interactions detection. On the basis of the scores obtained from the docking results, the interaction of (*E*)-*N*-(2-methylcinnamoyl)-amantadine with MAO-B was most favorable (score of −119.889, Figure 6). The second possibility not to be excluded is the interaction with COMT (−111.957). However, while for MAO-B, a hydrogen bonding interaction was detected for COMT, no hydrogen bonding interaction “enzyme ... ligand” was identified (Figure 7). Interestingly, the active sites of COMT and MAO-B shared a large amount of analogical AA and thus it may be possible to design a ligand that will interact with both enzymes.

Parkinson’s disease has high social significance, resulting from a progressive loss of nigrostriatal dopaminergic neurons. The decrease in striatal dopaminergic innervation due to this loss is responsible for motor disturbances characteristic of the disease, such as akinesia, muscular rigidity, and tremor, and cognitive function impairment later appears. Amantadine is an agent that raises the concentration of dopamine in the synaptic cleft in PD. Currently, levodopa is considered to be the gold standard for symptomatic treatment of PD. However, long-term treatment with levodopa is complicated by motor fluctuations and dyskinesia. Everything stated above requires the search for compounds that can replace levodopa and improve the efficacy of amantadine in the treatment of PD. In this line of thinking, we performed investigations of a newly obtained amantadine derivative CA(2-Me)-Am (3) on neuromuscular coordination, learning, and memory in an experimental mouse model of PD. The obtained data showed that amide 3 restored neuromuscular coordination and memory performance of parkinsonian animals to the control level, giving an indication of its beneficial protective effects.

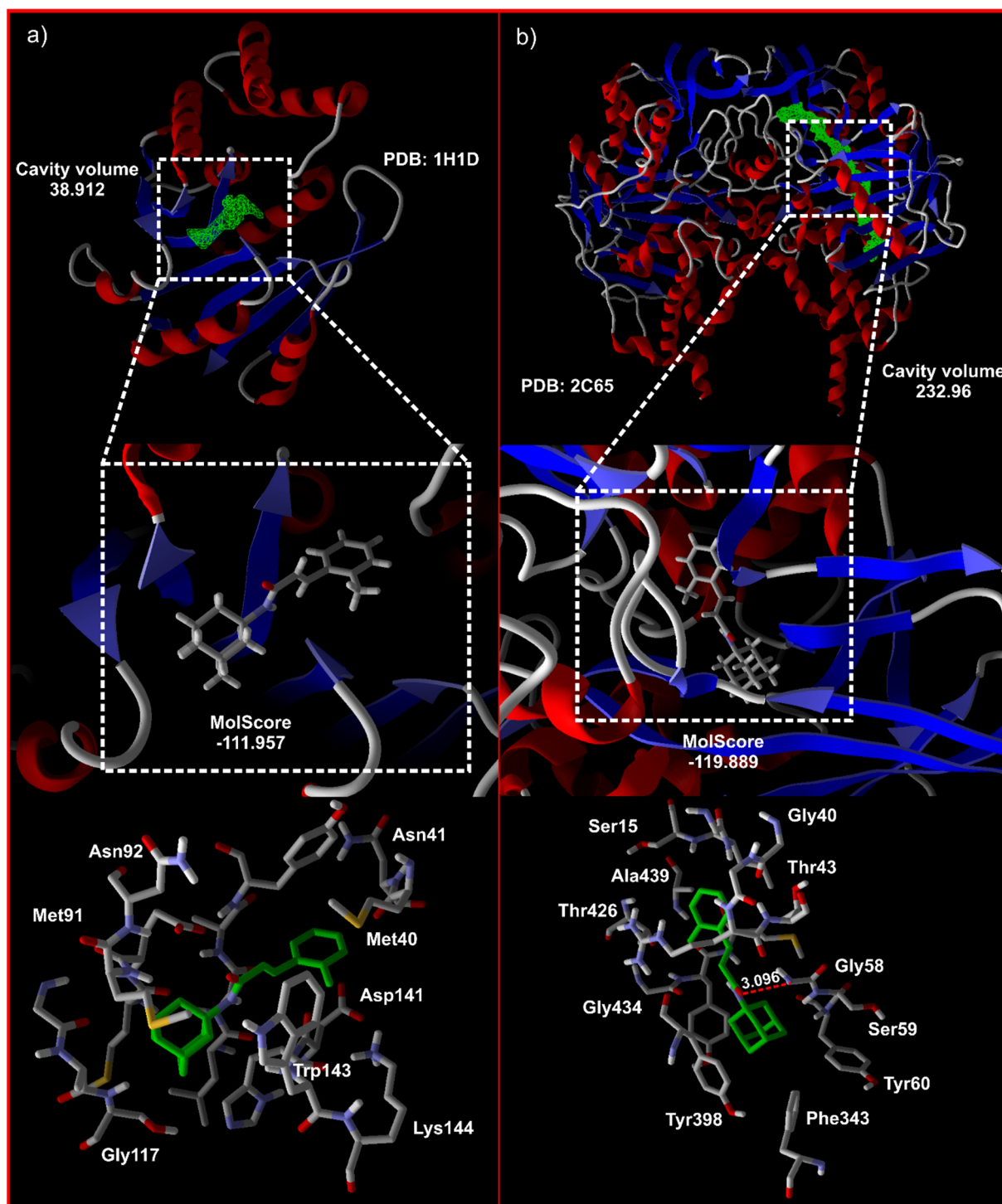


Figure 6. Visualization of the docking studies and molecular interaction of (*E*)-*N*-(2-methylcinnamoyl)-amantadine with (a) COMT and (b) MAO-B. The hydrogen bonding interaction *N*-H... O=C is shown in as red dashed line with the A... D distance of 3.096 Å.

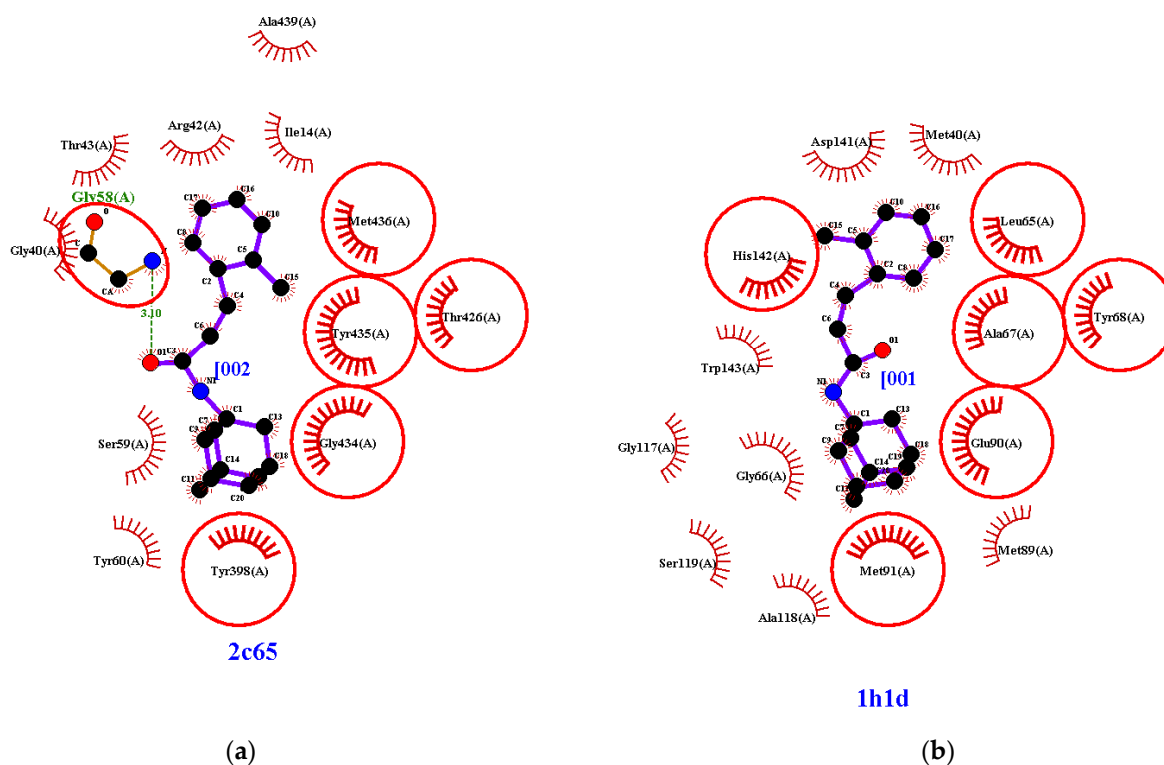


Figure 7. Observed interactions after docking of (*E*)-*N*-(2-methylcinnamoyl)-amantadine into the active site of two putative PD targets (a) MAO-B (2C65) and (b) COMT (1H1D). The hydrogen bonding interactions are shown in green; the hydrophobic contacts are shown as  for enzymes and with  for ligands; the similar residues for both enzymes are shown as .

Moreover, the molecular docking study investigations showed that from the considered four targets, (*E*)-*N*-(2-methylcinnamoyl)-amantadine interacted preferably with MAO-B, followed by COMT. The detected hydrogen bonding interaction could be used for development of modified potential antiviral drug candidates.

In conclusion, our results demonstrated ameliorating effects of the newly synthesized compound CA(2-Me)-Am in an experimental model of Parkinson's disease, which deserves further investigations.

Supplementary Materials: The following supporting information can be downloaded at: <https://www.mdpi.com/article/10.3390/cryst12111518/s1>, NMR and MS spectra of compound 3 are provided.

Author Contributions: Synthesis, supervision, writing and manuscript conceptualization, M.C.; NMR spectroscopy studies, N.P. and M.Š.; study, M.Š.; single crystal X-ray diffraction experiments, R.R. and H.S.-D.; docking studies, writing, B.S.; neurobehavioral studies, writing, R.K., L.T., M.L., A.P. and K.T. All authors have read and agreed to the published version of the manuscript.

Funding: This work was funded by the Bulgarian National Science Fund (BNSF), grant number KP-06-Russia/7-2019.

Institutional Review Board Statement: The animal study protocol was approved by the Commission of Bioethics (CBE) at the Institute of Neurobiology, Bulgarian Academy of Sciences—BAS/CBE/018/2020.

Informed Consent Statement: Not applicable.

Data Availability Statement: Crystallographic data for the structure of the title compound (*E*)-*N*-(2-methylcinnamoyl)-amantadine (CA(2-Me)-Am; 3)) was deposited in the CIF format with the Cambridge Crystallographic Data Center as 2205297. These data can be obtained free of charge via <http://www.ccdc.cam.ac.uk/conts/retrieving.html>, deposited on 05 September 2022 (or from the CCDC, 12 Union Road, Cambridge CB2 1EZ, UK; Fax: +441223336033; e-mail: deposit@ccdc.cam.ac.uk).

Conflicts of Interest: The authors declare no conflict of interest.

References

1. He, W.; Goodkind, D.; Kowal, P.R. *An Aging World: 2015*; International Population Reports; United States Census Bureau: Suitland-Silver Hill, MD, USA, 2016.
2. *Parkinson Disease: A Public Health Approach: Technical Brief*; World Health Organization: Geneva, Switzerland, 2022.
3. Mhyre, T.R.; Boyd, J.T.; Hamill, R.W.; Maguire-Zeiss, K.A. Parkinson's Disease. *Subcell. Biochem.* **2012**, *65*, 389–455. [[CrossRef](#)] [[PubMed](#)]
4. Wyss-Coray, T. Ageing, Neurodegeneration and Brain Rejuvenation. *Nature* **2016**, *539*, 180–186. [[CrossRef](#)] [[PubMed](#)]
5. Liu, J.; Obando, D.; Liao, V.; Lifa, T.; Codd, R. The Many Faces of the Adamantyl Group in Drug Design. *Eur. J. Med. Chem.* **2011**, *46*, 1949–1963. [[CrossRef](#)] [[PubMed](#)]
6. Wanka, L.; Iqbal, K.; Schreiner, P.R. The Lipophilic Bullet Hits the Targets: Medicinal Chemistry of Adamantane Derivatives. *Chem. Rev.* **2013**, *113*, 3516–3604. [[CrossRef](#)] [[PubMed](#)]
7. Schmidtke, M.; Zell, R.; Bauer, K.; Krumbholz, A.; Schrader, C.; Suess, J.; Wutzler, P. Amantadine Resistance among Porcine H1N1, H1N2, and H3N2 Influenza A Viruses Isolated in Germany between 1981 and 2001. *Intervirology* **2006**, *49*, 286–293. [[CrossRef](#)]
8. Nelson, M.I.; Simonsen, L.; Viboud, C.; Miller, M.A.; Holmes, E.C. The Origin and Global Emergence of Adamantane Resistant A/H3N2 Influenza Viruses. *Virology* **2009**, *388*, 270–278. [[CrossRef](#)]
9. Weinstock, D.M.; Zuccotti, G. The Evolution of Influenza Resistance and Treatment. *JAMA* **2009**, *301*, 1066–1069. [[CrossRef](#)]
10. Schwab, R.S.; England, A.C.; Poskanzer, D.C.; Young, R.R. Amantadine in the Treatment of Parkinson's Disease. *JAMA* **1969**, *208*, 1168–1170. [[CrossRef](#)]
11. Rascol, O.; Fabbri, M.; Poewe, W. Amantadine in the Treatment of Parkinson's Disease and Other Movement Disorders. *Lancet Neurol.* **2021**, *20*, 1048–1056. [[CrossRef](#)]
12. Adisakwattana, S. Cinnamic Acid and Its Derivatives: Mechanisms for Prevention and Management of Diabetes and Its Complications. *Nutrients* **2017**, *9*, E163. [[CrossRef](#)]
13. Liu, L.; Hudgins, W.R.; Shack, S.; Yin, M.Q.; Samid, D. Cinnamic Acid: A Natural Product with Potential Use in Cancer Intervention. *Int. J. Cancer* **1995**, *62*, 345–350. [[CrossRef](#)]
14. Prorok, T.; Jana, M.; Patel, D.; Pahan, K. Cinnamic Acid Protects the Nigrostriatum in a Mouse Model of Parkinson's Disease via Peroxisome Proliferator-Activated Receptor α . *Neurochem. Res.* **2019**, *44*, 751–762. [[CrossRef](#)]
15. Hemmati, A.A.; Alboghobeish, S.; Ahangarpour, A. Effects of Cinnamic Acid on Memory Deficits and Brain Oxidative Stress in Streptozotocin-Induced Diabetic Mice. *Korean J. Physiol. Pharmacol. Off. J. Korean Physiol. Soc. Korean Soc. Pharmacol.* **2018**, *22*, 257–267. [[CrossRef](#)]
16. Knorr, R.; Trzeciak, A.; Bannwarth, W.; Gillessen, D. New Coupling Reagents in Peptide Chemistry. *Tetrahedron Lett.* **1989**, *30*, 1927–1930. [[CrossRef](#)]
17. Rigaku Oxford Diffraction. CrysAlis pro. Rigaku Oxford Diffraction, CrysAlis pro CrysAlis Pro. 2015. Available online: <https://www.rigaku.com/products/crystallography/crysalis> (accessed on 20 October 2022).
18. Sheldrick, G.M. SHELXT-Integrated Space-Group and Crystal-Structure Determination. *Acta Crystallogr. Sect. Found. Adv.* **2015**, *71*, 3–8. [[CrossRef](#)]
19. Sheldrick, G.M. A Short History of SHELX. *Acta Crystallogr. A* **2008**, *64*, 112–122. [[CrossRef](#)]
20. Shin, K.S.; Zhao, T.T.; Choi, H.S.; Hwang, B.Y.; Lee, C.K.; Lee, M.K. Effects of Gypenosides on Anxiety Disorders in MPTP-Lesioned Mouse Model of Parkinson's Disease. *Brain Res.* **2014**, *1567*, 57–65. [[CrossRef](#)]
21. Manna, S.; Bhattacharyya, D.; Mandal, T.K.; Dey, S. Neuropharmacological Effects of Deltamethrin in Rats. *J. Vet. Sci.* **2006**, *7*, 133–136. [[CrossRef](#)]
22. Shahidi, S.; Komaki, A.; Mahmoodi, M.; Atrvash, N.; Ghodrati, M. Ascorbic Acid Supplementation Could Affect Passive Avoidance Learning and Memory in Rat. *Brain Res. Bull.* **2008**, *76*, 109–113. [[CrossRef](#)]
23. Land, M.A.; Robertson, K.N.; Ylijoki, K.E.O.; Clyburne, J.A.C. Reactivity of 1,3-Dichloro-1,3-Bis(Dimethylamino)-Propenium Salts with Primary Amines. *New J. Chem.* **2021**, *45*, 13558–13570. [[CrossRef](#)]
24. Pereira, A.K.d.S.; Manzano, C.M.; Nakahata, D.H.; Clavijo, J.C.T.; Pereira, D.H.; Lustri, W.R.; Corbi, P.P. Synthesis, Crystal Structures, DFT Studies, Antibacterial Assays and Interaction Assessments with Biomolecules of New Platinum (II) Complexes with Adamantane Derivatives. *New J. Chem.* **2020**, *44*, 11546–11556. [[CrossRef](#)]
25. Perlovich, G.L.; Ryzhakov, A.M.; Tkachev, V.V.; Hansen, L.K.; Raevsky, O.A. Sulfonamide Molecular Crystals: Structure, Sublimation Thermodynamic Characteristics, Molecular Packing, Hydrogen Bonds Networks. *Cryst. Growth Des.* **2013**, *13*, 4002–4016. [[CrossRef](#)]

26. Sarcevic, I.; Orola, L.; Veidis, M.V.; Podjava, A.; Belyakov, S. Crystal and Molecular Structure and Stability of Isoniazid Cocrystals with Selected Carboxylic Acids. *Cryst. Growth Des.* **2013**, *13*, 1082–1090. [[CrossRef](#)]
27. Swapna, B.; Maddileti, D.; Nangia, A. Cocrystals of the Tuberculosis Drug Isoniazid: Polymorphism, Isostructurality, and Stability. *Cryst. Growth Des.* **2014**, *14*, 5991–6005. [[CrossRef](#)]
28. Etter, M.C.; MacDonald, J.C.; Bernstein, J. Graph-Set Analysis of Hydrogen-Bond Patterns in Organic Crystals. *Acta Crystallogr. B* **1990**, *46*, 256–262. [[CrossRef](#)]
29. Etter, M.C. Encoding and Decoding Hydrogen-Bond Patterns of Organic Compounds. *Acc. Chem. Res.* **1990**, *23*, 120–126. [[CrossRef](#)]
30. Farrugia, L.J. WinGX and ORTEP for Windows: An Update. *J. Appl. Crystallogr.* **2012**, *45*, 849–854. [[CrossRef](#)]
31. Jaakola, V.-P.; Griffith, M.T.; Hanson, M.A.; Cherezov, V.; Chien, E.Y.T.; Lane, J.R.; Ijzerman, A.P.; Stevens, R.C. The 2.6 Angstrom Crystal Structure of a Human A2A Adenosine Receptor Bound to an Antagonist. *Science* **2008**, *322*, 1211–1217. [[CrossRef](#)]
32. Bonifácio, M.J.; Archer, M.; Rodrigues, M.L.; Matias, P.M.; Learmonth, D.A.; Carrondo, M.A.; Soares-Da-Silva, P. Kinetics and Crystal Structure of Catechol-o-Methyltransferase Complex with Co-Substrate and a Novel Inhibitor with Potential Therapeutic Application. *Mol. Pharmacol.* **2002**, *62*, 795–805. [[CrossRef](#)]
33. Binda, C.; Hubálek, F.; Li, M.; Herzig, Y.; Sterling, J.; Edmondson, D.E.; Mattevi, A. Binding of Rasagiline-Related Inhibitors to Human Monoamine Oxidases: A Kinetic and Crystallographic Analysis. *J. Med. Chem.* **2005**, *48*, 8148–8154. [[CrossRef](#)]
34. Chou, T.-H.; Epstein, M.; Michalski, K.; Fine, E.; Biggin, P.C.; Furukawa, H. Structural Insights into Binding of Therapeutic Channel Blockers in NMDA Receptors. *Nat. Struct. Mol. Biol.* **2022**, *29*, 507–518. [[CrossRef](#)]
35. Pettersen, E.F.; Goddard, T.D.; Huang, C.C.; Couch, G.S.; Greenblatt, D.M.; Meng, E.C.; Ferrin, T.E. UCSF Chimera—a Visualization System for Exploratory Research and Analysis. *J. Comput. Chem.* **2004**, *25*, 1605–1612. [[CrossRef](#)]
36. Wallace, A.C.; Laskowski, R.A.; Thornton, J.M. LIGPLOT: A Program to Generate Schematic Diagrams of Protein-Ligand Interactions. *Protein Eng. Des. Sel.* **1995**, *8*, 127–134. [[CrossRef](#)]